journal

J. Am. Ceram. Soc., 78 [7] 1935-39 (1995)

Epitaxial Aluminum-Doped Zinc Oxide Thin Films on Sapphire: II, Defect Equilibria and Electrical Properties

V. Srikant, Valter Sergo,* and David R. Clarke*

Department of Materials, University of California, Santa Barbara, California 93106-5050

The electrical transport properties of epitaxial ZnO films grown on different orientations of sapphire substrates have been measured as a function of partial pressure of oxygen. After equilibration, the carrier concentration is found to change from a $p_{O_2}^{-1/4}$ to a $p_{O_2}^{-3/8}$ dependence with increasing oxygen partial pressure. The partial pressure dependence is shown to be consistent with zinc vacancies being the rate-controlling diffusive species. In addition, the carrier concentration in ZnO films grown on A-, C-, and M-plane sapphire are the same but that of R-plane sapphire is systematically lower. Electron Hall mobility measurements as a function of carrier concentration for all the substrate orientations exhibit a transition from "single-crystal" behavior at high carrier concentrations to "polycrystalline" behavior at low carrier concentrations. This behavior is attributed to the effective height of potential barriers formed at the low-angle grain boundaries in the epitaxial ZnO films. The trap density at the grain boundaries is deduced to be ~7 × 10^{12}/cm^2. The electron mobility, at constant carrier concentration, varies with the substrate orientation on which the ZnO films were grown. The difference is attributed to the difference in dislocation density in the films produced as a result of lattice mismatch with the different sapphire orientations.

I. Introduction

THIN films of zinc oxide are increasingly being used[1-3] in chemical sensors, in surface acoustic wave (SAW) devices, and in a variety of novel devices utilizing the unique combination of piezoelectric, conducting, and optical properties of ZnO. Aluminum doping of zinc oxide thin films increases their conductivity without impairing their optical transmission until very high doping concentrations.[4] As a result, Al-doped ZnO thin films have attracted considerable attention for their potential as transparent conducting electrodes in displays. Much of this attention has been directed toward achieving the best combination of electrical and optical properties of Al-doped ZnO films on glass substrates. There has also been some work devoted to achieving epitaxy of ZnO on sapphire by various growth techniques but there is a paucity of information regarding the electrical properties of Al-doped ZnO films grown on sapphire substrates. As mentioned in Part I, our interest in ZnO films, in part, is to gain further insight into the varistor behavior in ZnO ceramics by studying bicrystal films of different crystallographic misorientations. This requires a knowledge of well-characterized oriented single-crystal Al-doped ZnO films. In Part I we described the growth conditions and the epitaxial relationships achieved between ZnO films and different orientations of sapphire. An important characteristic of the films is that although they are epitaxial they also have a slight mosaic structure consisting of oriented grains separated by low-angle (~1°) grain or sub-grain boundaries. Here in Part II we evaluate the defect equilibria that control the observed electrical conductivity and report on the electrical properties of the films on different orientations of sapphire substrates.

S.-I. Hirano—contributing editor

Manuscript No. 193181. Received September 28, 1994; approved February 20, 1995.

This work was supported by the Department of Energy, Office of Basic Energy Sciences, under Grant No. DE-FG03-91ER45447. Additional support for V. Sergo was provided by the Italian National Research Council.

*Member, American Ceramic Society.

II. Experimental Details

(1) *Growth of Films*

The Al-doped ZnO films were grown by pulsed laser ablation in a turbo-pumped vaccum chamber using a frequency-tripled, Q-switched Nd:YAG laser. The full details are described in Part I.[5] All of the samples tested were grown at a substrate temperature of 600°C and a background pressure of oxygen of 10 mtorr unless otherwise stated. The thickness of all of the films studied was ~0.12 μm as measured by ellipsometry.

(2) *Electrical Measurements*

The electronic conductivity and electron mobility of the films were measured at room temperature using a standard van der Pauw four-probe square geometry. Electrical contact was made using pads of indium, which is known to form good ohmic contact with ZnO.[6] The Hall effect measurements were performed at a magnetic field induction of about 1 T. The carrier concentration and the Hall mobility were measured at a current of 1 mA. Typically, five different measurements were made on each film after each heat treatment. The samples used were in the form of 5 × 5 mm squares.

(3) *Oxygen Partial Pressure Dependence*

In order to evaluate the defect equilibrium in Al-doped ZnO films, the carrier concentration as a function of partial pressure of oxygen was investigated. This was accomplished by annealing the films at different oxygen partial pressures in a vacuum chamber at 750°C. The oxygen partial pressure during annealing could be varied from 0.005 to 500 mtorr.

Because of the very high energy of the ablated species, the defect concentration (and hence the carrier concentration) incorporated in the as-grown film is in excess of the equilibrium value. Hence, any equilibrium analysis on the as-grown films would be in error. With this in mind, the films were subject to a high-temperature anneal before using them for further analysis. Two samples were chosen to determine the annealing time required to reach equilibrium at a given oxygen partial pressure. One sample was grown on A-plane sapphire and subsequently annealed at 750°C in 10 mtorr of oxygen. The other was grown on M-plane sapphire and subsequently annealed at 750°C in 1 mtorr of oxygen. In either case, a steady-state value of the carrier concentration was reached within 1 h of annealing. Having achieved an equilibrium concentration of defects as evidenced by the carrier concentration, these samples were then subject to a series of anneals at 750°C. The film on the A-plane was annealed at 500 mtorr, whereas the film on the M-plane was annealed at 100 mtorr of oxygen. The carrier concentration

was measured periodically to determine the annealing time required to achieve a steady-state value.

III. Results

(1) Equilibration

These experiments were carried out to determine the annealing time required to reach an equilibrium defect concentration in the ZnO films at an annealing temperature of 750°C. As will be discussed, they also provide information on the rate-controlling diffusing species for defect equilibria in ZnO thin films.

In Fig. 1 the measured carrier concentration is plotted as a function of annealing time for Al-doped zinc oxide films on A- and M-plane sapphire. The solid triangles and circles indicate measured carrier concentration for films grown on M-plane and A-plane sapphire, respectively. As indicated, ZnO films on both A- and M-plane sapphire were found to reach equilibrium carrier concentration within 5 h of annealing. Hence, all subsequent annealing, to attain equilibrium carrier concentration at a given oxygen partial pressure, was conducted for 5 h.

(2) Oxygen Partial Pressure Dependence of Carrier Concentration

The carrier concentration as a function of oxygen partial pressure is plotted in Fig. 2 for ZnO films grown on different sapphire substrates. All of the films were grown under the standard conditions except for the ZnO film on R-plane, which was grown at a higher substrate temperature of 750°C so as to form an epitaxial film with an a-axis orientation. Over the range of partial pressures investigated, two different electroneutrality conditions appear to prevail on all of the films, described by slopes of $-1/4$ and $-3/8$. It is also observed that the films on R-plane sapphire show a lower carrier concentration at all oxygen partial pressures compared to c-axis oriented films grown on A-, M-, and C-plane sapphire.

(3) Carrier Concentration vs Mobility

As shown in the previous section, the carrier concentration could be altered over a large range (3×10^{18}–1×10^{20}/cm^3) by annealing the films under different oxygen partial pressures. The electron Hall mobility also changed and is plotted in Fig. 3 as a function of carrier concentration for films grown on the A-, M-, R-plane sapphire. For comparison, the published data of the electron mobility of single-crystal ZnO as a function of carrier concentration is also plotted.[7] The thin lines joining the experimental points are a guide to the eye. It is observed that for a given carrier concentration, the Hall mobilities of the films are lower than those realized in doped single-crystal ZnO. It is also observed that for carrier concentrations greater than 2×10^{19}/cm^3 the films on the different substrates behave like a "single crystal" as evidenced by the similar slopes. On the other hand, a dramatic decrease in the Hall mobility of the films grown on the different substrates is observed for carrier concentrations less than 2×10^{19}/cm^3.

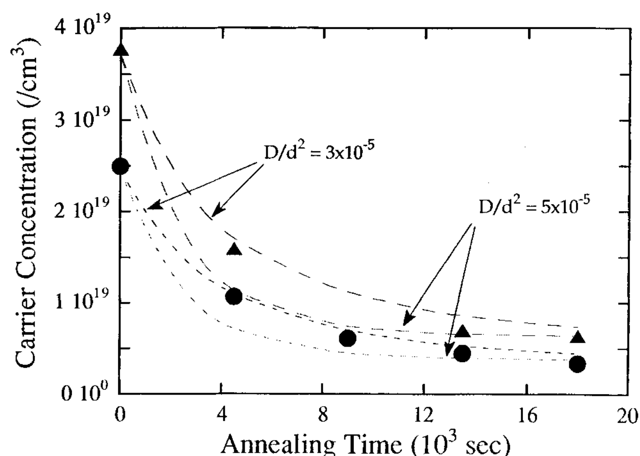

Fig. 1. Measured carrier concentration as a function of annealing time at 750°C for epitaxial ZnO films grown on M-plane and A-plane sapphire. The curves superimposed on the data are lines corresponding to different values of the diffusion coefficient normalized by the square of the grain size, as explained in the text.

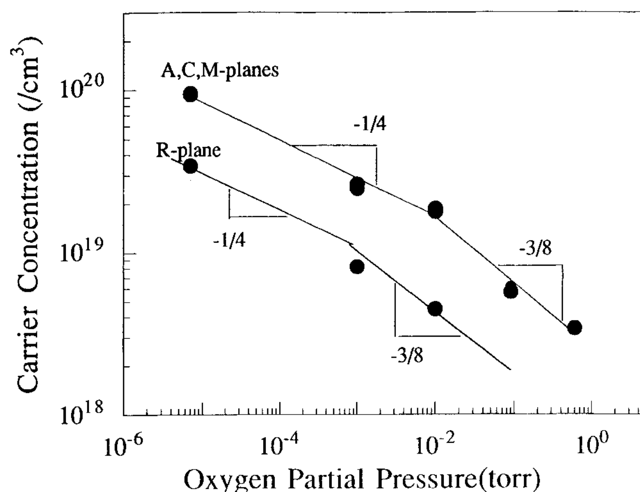

Fig. 2. Equilibrium carrier concentration as a function of oxygen partial pressure after annealing at 750°C. The data for the ZnO films grown on A-, C-, and M-plane sapphire are indistinguishable. The thin lines correspond to the partial pressure dependencies obtained from the neutrality conditions described in Table II. The error in measurement is equal to or less than the symbol size.

IV. Discussion

The experimental findings indicate that the electrical transport properties of our epitaxial ZnO films depend strongly on the partial pressure of oxygen and, to a lesser but still significant extent, on the orientation of the sapphire substrate onto which the films were grown. In the following, we will relate the observed dependence of the carrier concentration on the oxygen

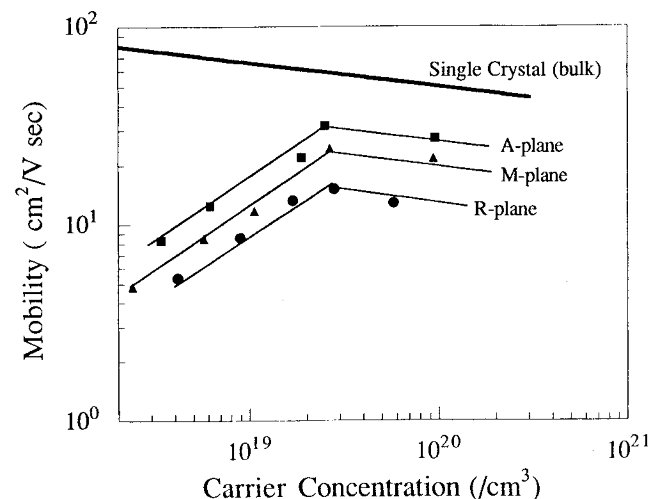

Fig. 3. Electron mobility as a function of the carrier concentration. The ZnO films grown on the A-, M-, and R-plane sapphire substrates exhibit a transition from polycrystalline to single-crystal behavior at the same carrier concentration. The difference in mobility for films grown on different substrate orientations is attributed to the difference in dislocation density arising from the lattice mismatch with the substrates. Again the error in measurement is equal to or less than the symbol size.

Table I. Relevant Quasi-chemical Defect Reactions Used to Evaluate Carrier Concentrations as a Function of Oxygen Partial Pressure of Al-Doped ZnO Films

Quasi-chemical reactions	Mass action relationship
Frenkel disorder	
$Zn_{Zn} = Zn_i^x + V_{Zn}^x$	$[Zn_i^x][V_{Zn}^x] = K_F$
Intrinsic electronic disorder	
$nil = e' + h^{\cdot}$	$np = K_i$
Reduction	
$Zn_{Zn} + O_O = Zn_i^x + \frac{1}{2}O_2(g)$	$[Zn_i^x]P_{O_2}^{1/2} = K_R$
Oxidation	
$\frac{1}{2}O_2(g) = O_O + V_{Zn}^x$	$[V_{Zn}^x]P_{O_2}^{-1/2} = K_O$
ZnO vaporization	
$Zn_{Zn} + O_O = Zn(g) + \frac{1}{2}O_2(g)$	$P_{Zn}P_{O_2}^{1/2} = K_{ZnO}$
Acceptor ionization	
$V_{Zn}^x = V_{Zn}' + h^{\cdot}$	$[V_{Zn}']p/[V_{Zn}^x] = K_1$
$V_{Zn}' = V_{Zn}'' + h^{\cdot}$	$[V_{Zn}'']p/[V_{Zn}'] = K_2$
Dopant reaction	
$Al_2O_3 + 2Zn_{Zn} = 2Al_{Zn}^x + 2Zn_i^x + \frac{3}{2}O_2(g)$	$[Al_{Zn}^x]^2[Zn_i^x]^2P_{O_2}^{3/2} = K_3$
$Al_2O_3{\cdot}ZnO + 2Zn_{Zn} = 2Al_{Zn}^x + 2Zn_i^x + \frac{3}{2}O_2(g) + ZnO$	$[Al_{Zn}^x]^2[Zn_i^x]^2P_{O_2}^{3/2} = K_3$
Dopant/Donor ionization	
$Al_{Zn}^x = Al_{Zn}^{\cdot} + e'$	$[Al_{Zn}^{\cdot}]n/[Al_{Zn}^x] = K_4$

partial pressure to defect equilibria. Then, we relate the mobility dependence on the carrier concentration to standard models of electrical transport in polycrystalline semiconductors, the assumption being that although the ZnO films are epitaxial, their mosaic structure is a result of the presence of small-angle grain boundaries which behave as potential barriers to electrical transport.

In relating the carrier concentration to the oxygen partial pressure, the partial pressure dependence has been considered in terms of the equilibrium of simple intrinsic and extrinsic defects. The relevant quasi-chemical reactions and the corresponding mass action relationships are listed in Table I. In writing these reactions, we have assumed that the Al doping levels are so high that they are the dominant donor reaction. This assumption is consistent with the observation that the carrier concentrations in our films are at least 2 orders of magnitude higher than those realized at the same oxygen partial pressures in undoped ZnO.[8] By applying the different electroneutrality conditions to the equations listed in Table I, the partial pressure dependencies associated with the neutrality conditions in Table II are obtained. By comparison with the observed slopes in Fig. 2, the oxygen partial pressure dependencies predicted for the neutrality conditions, $[Al_{Zn}^{\cdot}] = 2[V_{Zn}'']$ and $[Al_{Zn}^{\cdot}] = [V_{Zn}']$, are seen to pertain. This then suggests that as the oxygen partial pressure is varied, equilibrium in defect concentration is obtained by adjusting the concentration of singly and doubly ionized zinc vacancies in the grains. As the films have a mosaic structure with small-angle grain boundaries perpendicular to the film surface, it is expected that as the oxygen partial pressure is changed, equilibration is accomplished by the diffusion of zinc vacancies from the free surface and from the grain boundaries into the interior of the grains.

Additional, albeit indirect, evidence for the rate-controlling species being zinc vacancies comes from the following consistency argument based on the rates of equilibration of the carrier concentration shown in Fig. 1. We assume that when the oxygen partial pressure is changed, transport along the grain boundaries is rapid and that equilibration is then controlled by the diffusion of a species laterally from the grain boundaries into the center of the grains. The time of equilibration is then expected to be dependent on the size of the grains, d, and the effective diffusion coefficient, D. On the basis of this expectation, two-dimensional diffusion curves, corresponding to different values of D/d^2, are superimposed on the experimental data of Fig. 1. For both films grown on M- and A-plane sapphire, the annealing time dependence corresponds to values of D/d^2 lying between 3×10^{-5} and 5×10^{-5} per second. Using these values, we may compare the grain size and effective diffusion coefficient that are consistent with the observed equilibration. This comparison is shown in Fig. 4 with the lines of constant D/d^2 for values of 3×10^{-5} and 5×10^{-5} per second. Also shown in Fig. 4, as shaded blocks on the top axis, are the range of values reported for the diffusion coefficients at 750°C for Zn interstitials, Zn vacancies, and oxygen vacancies.[9] The corresponding grain sizes consistent with the reported diffusion coefficients, as well as the lines of constant D/d^2 that are consistent with our equilibration times, would be 0.1–1 nm, 100–500 nm, and 0.5–1 mm if V_O, V_{Zn}, and Zn_i, respectively, were the rate-controlling diffusing species. Since the smallest and largest values are incompatible with the expected grain sizes of our films, whereas the intermediate value is, we conclude that zinc vacancies are indeed the rate-controlling diffusing species.

A notable feature of the data presented in Fig. 2 is that whereas the Al-doped ZnO films grown on A-, M-, and C-plane sapphire have similar characteristics, the films grown on R-plane sapphire have a lower carrier concentration at all oxygen partial pressures. As the films grown on A-, M-, and C-plane sapphire are c-axis oriented, whereas the films grown on R-plane sapphire are a-axis oriented, the distinction appears to be between c-axis and a-axis oriented films. The most obvious explanation is that the lower carrier concentration in the R-plane films is due to a lower incorporation of Al ions during growth on this plane. This would then imply, from the defect equations developed earlier, that the transition from the electroneutrality condition $[Al_{Zn}^{\cdot}] = 2[V_{Zn}'']$ to $[Al_{Zn}^{\cdot}] = [V_{Zn}']$ would occur at a lower oxygen partial pressure for films grown on R-plane as compared to those grown on A-, M-, or C-plane. This is the behavior exhibited in Fig. 2. At the present, the exact reason for the lower incorporation of Al into the films grown on R-plane is not known. However, one possibility is that the formation energy for creating a vacancy on the surface of a-axis films is smaller than on the surface of c-axis films. This would

Table II. Possible Neutrality Conditions and the Calculated Partial Pressure Dependencies of the Carrier Concentration in Those Regimes Based on the Defect Equations Listed in Table I

Neutrality condition	Partial pressure dependence
$[Al_{Zn}^{\cdot}] = n$	$n \propto P_{O_2}^{-1/8}$
$[Al_{Zn}^{\cdot}] = 2[V_{Zn}'']$	$n \propto P_{O_2}^{-1/4}$
$[Al_{Zn}^{\cdot}] = [V_{Zn}']$	$n \propto P_{O_2}^{-3/8}$

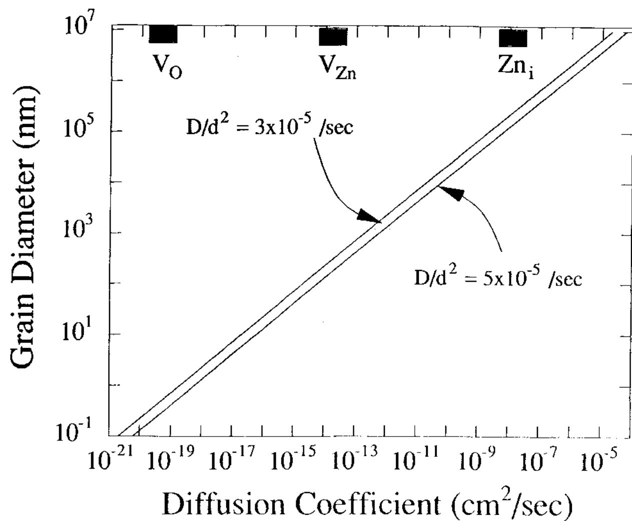

Fig. 4. Grain diameter versus effective diffusion coefficient. The values of D/d^2 that fit the equilibration carrier concentration data in Fig. 1 are shown, as are the reported values for the diffusion coefficients for oxygen vacancies, zinc vacancies, and zinc interstitials.

be analogous to the observation by McVicker *et al.*[10] that the sublimation energy is different for the two (dissimilar) polar surfaces of ZnO.

The mobility dependence on carrier concentration shown in Fig. 3 exhibits a number of intriguing features. First, the mobility increases and then decreases with increasing carrier concentration. This trend occurs irrespective of the substrate orientation. Interestingly, in the high carrier concentration regime ($n > 2 \times 10^{19}$–$3 \times 10^{19}/\text{cm}^3$) the slope of the electron mobility against carrier concentration is the same for our ZnO films as for ZnO single crystals. The implication of this is that in the high carrier concentration regime, the electrical transport in the films is similar to that in a single crystal, whereas in the low carrier concentration regime it is not. Second, the apparent discontinuity in mobility dependence occurs at the same carrier concentration irrespective of the substrate orientation. Third, the magnitude of the electron mobility depends on the substrate orientation onto which the films were grown rather than the crystallographic orientation of the film itself.

These observations of effective electron mobility can be understood within the established framework[11–15] of electrical transport in polycrystalline semiconductors that have potential barriers at their grain boundaries (Fig. 5). In modeling the conductivity, defects are localized at the grain boundaries and act as traps for the majority carriers from the adjoining grains.[14–15] The trapped electrons set up a negative charge at the grain boundaries which gives rise to a space charge region in the grains due to the accumulation of counterions having a positive charge, namely the donor atoms. This produces a potential barrier at the grain boundaries that resembles a back-to-back Schottky barrier and impedes the motion of electrons when a voltage is applied across the polycrystalline material. The identity of the localized traps in our films is not known. However, the mosaic structure indicates that the films contain low-angle twist and tilt grain boundaries which are believed to contain defect states within the band gap. These may be intrinsic, resulting from the geometrical arrangement of ions at the grain boundaries or the formation of grain boundary dislocations, or extrinisic due to doping. (Recent work,[16] in which bismuth is diffused along the grain boundaries in our films, indicates that a large density of defect states can be created extrinsically.)

The detailed description of the potential distribution, and hence the conductivity, in a polycrystalline semiconductor with electrical barriers at the grain boundaries depends on the relative scale of the electron mean free path, the extent of the space charge region (depletion width) and the grain size, as well as on the carrier concentration and the density and energy of the interface states. One approach is to assume a constant grain size and solve for the potential, in one dimension, due to a periodic spacing of potential barriers at the boundaries.[12] Alternatively, if the electron mean free path and the Debye length are much less than the grain size, one can make the abrupt junction approximation[13] and consider the effect of a single, isolated grain boundary. The electron mean free path (λ_e) can be expressed as

$$\lambda_e = \frac{\mu m^* c}{e} \tag{1}$$

Using published data for the effective mass, m^*, and mobility, μ, for ZnO,[6,9] we obtain a value for the mean free path of ~3 nm. This is much smaller than the grain size (100–500 nm) in our epitaxial, laser ablated films. This suggests that the abrupt junction approximation is valid. Another important consideration is the size of the depletion width (W), which can be determined from the electroneutrality condition:

$$N_S = 2nW \tag{2}$$

where N_S = density of traps at the grain boundary (cm^{-2}) and n = carrier concentration in the grain (cm^{-3}). As we have no *a priori* knowledge of the trap density at the grain boundaries, we cannot uniquely determine the depletion width. Hence, we consider two possibilities,

$W < d/2$ (case I)

$W > d/2$ (case II)

where d is the grain size. For case I, it is reasonable to assume that the carrier density in the grain is a constant and mobility is thermally activated.[11] However, for case II the above assumption is valid only if the Debye length

$$L_D = \left[\frac{\varepsilon\varepsilon_0 kT}{ne^2}\right]^{1/2} \tag{3}$$

is smaller than the grain size.[11] For the present case, the Debye

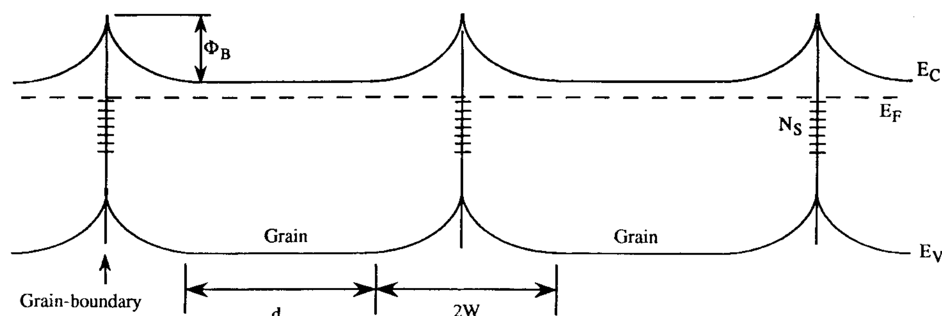

Fig. 5. Schematic band structure diagram for a polycrystalline ZnO film having periodic spaced and charged grain boundaries. The different symbols are introduced in the text.

length is calculated to be about 3 nm, which is again much smaller than the expected grain size in our films. Hence, we again conclude that for the ZnO films grown in this study the abrupt junction approximation is justified and in addition that the carrier concentration measured by the Hall effect is the bulk carrier density and the electron mobility is thermally activated.

Based on the numerical calculations of Evans and Nelson[17] and the carrier concentrations of our films, we can make the assumption that thermionic emission is the rate-limiting step for electron transport across the grain boundaries. If we further assume that even for the lowest carrier concentrations measured, all of the interface states are filled, i.e., there are no energy states above the Fermi level at the grain boundary, then the interface charge can be considered a constant. Finally, we assume that the potentials at all of the grain boundaries are identical. Together, these assumptions allow, the simplest one-dimensional model, the abrupt junction model, for electron transport across grain boundaries, to be used. By solving the Poisson equation for the donor distribution in the vicinity of the grain boundaries and applying the condition of charge neutrality (Eq. (2)), the barrier height, Φ_B, carrier concentration, n, density of interface states, and the mobility are related by the following:

$$\Phi_B = \frac{eN_S^2}{2\varepsilon\varepsilon_0 n} - \frac{kT}{e} \quad (4)$$

$$\mu = \mu_0 \exp\left(-\frac{\Phi_B}{kT}\right) \quad (5)$$

where ε is the dielectric constant of the grains, μ is the activated mobility, and $\mu_o = q\bar{c}d'/8kT$, where $d' = d + d_1$ and d_1 is the grain boundary thickness. Equation (4) is also the same as used by Heywang[18] and Jonker[19] in their analyses of the effect of resistive grain boundaries in PTC semiconducting barium titanate.

These relationships above provide the basis for understanding the mobility data presented in Fig. 3. At large carrier concentrations, the barrier height becomes negligible in comparison with the thermal energy kT (Eq. (4)). As a consequence, in this regime of carrier concentration, the electron mobility is expected to depend on carrier concentration in the same way as that of a single crystal. At low carrier concentrations, the barrier height increases with decreasing carrier concentrations. As a result, the effective mobility in this regime decreases with decreasing carrier concentration. There is thus a crossover in mobility dependence between "single-crystal" and "polycrystalline" behavior according to whether the grain boundary barrier height is less than or more than a critical value. From the experimental data, this threshold occurs at a value of carrier concentration, n_C, of about 2×10^{19}–3×10^{19}/cm^3. Assuming this occurs when the barrier height is approximately equal to $2kT$, then by combining Eqs. (2) and (4) and rewriting in terms of depletion width we have

$$w = \frac{N_S}{2n_C} = \left[\frac{16\varepsilon\varepsilon_0 kT}{n_C e^2}\right]^{1/2}$$

Substituting in numerical values, the effective depletion width at the threshold carrier concentration is 2.5–3.1 nm. Using Eq. (2), this then leads to an effective grain boundary trap density of between 6.2×10^{12} and 7.6×10^{12}/cm^2.

The barrier model presented does not explain the obvious difference in mobility, at constant carrier concentration, between the films grown on different orientations of sapphire substrates, as well as the overall lower mobilities observed in the films in comparison to the reported values for single-crystal ZnO. The fact that the threshold carrier concentration is the same for all of the films and they have the same thickness suggests that the mobility difference is not due to the properties of the grain boundaries but rather is a result of differences in the mobility within the grains themselves, probably caused by electron scattering from dislocations in the grains. As the orientation of the films on the A-, M-, and C-sapphire substrates is all the same, we attribute the differences to differences in the dislocation density in the films. Specifically, as the geometrical mismatch between the films and the substrate are expected to depend on the substrate orientation, we conclude that the overall mobility decreases with increasing lattice mismatch between the ZnO films and the substrate.

References

[1] F. C. M. Van de Pol, "Thin Film ZnO—Properties and Applications," *Am. Ceram. Soc. Bull.*, **69** [12] 1959–65 (1990).

[2] D. L. Polla, R. S. Muller, and R. M. White, "Integrated Multisensor Chip," *IEEE Electron Device Lett.*, **7** [4] 254–56 (1986).

[3] A. L. Farenbruch and R. H. Bube, *Fundamentals of Solar Cells*. Academic Press, New York, 1983.

[4] Z. C. Jin, I. Hamberg, and C. G. Granqvist, "Optical Properties of Sputter-Deposited ZnO:Al Thin Films," *J. Appl. Phys.*, **64** [10] 5117–31 (1988).

[5] V. Srikant, V. Sergo, and D. R. Clarke, "Epitaxial Al-Doped Zinc Oxide Thin Films on Sapphire: I, Effect of Substrate Orientation," *J. Am. Ceram. Soc.*, **78** [7] 1931–34 (1995).

[6] A. R. Hutson, "Hall Effect Studies of Doped Zinc Oxide Single Crystals," *Phys. Rev.*, **108** [2] 222–30 (1957).

[7] G. Heiland, E. Mollow, and F. Stockmann, "Electronic Processes in Zinc Oxide," *Solid State Phys.*, **8**, 191–323 (1959).

[8] J. S. Choi and C. H. Yo, "Study of the Nonstoichiometric Composition of Zinc Oxide," *J. Chem. Phys.*, **37**, 1149–51 (1976).

[9] Landolt-Bornstein, *Semiconductors*, Vol. 17; pp. 35–60. Springer-Verlag, Berlin, Germany, 1982.

[10] J. E. McVicker, R. A. Rapp, and J. P. Hirth, "The Sublimation of Basal Surfaces of Zinc Oxide," *J. Chem. Phys.*, **63** [6] 2646–58 (1975).

[11] J. W. Orton and M. J. Powell, "The Hall Effect in Polycrystalline and Powdered Semiconductors," *Rep. Prog. Phys.*, **43**, 1263–305 (1980).

[12] H. J. Moller and V. Schlichting, "Measurement and Calculation of the Carrier Concentration in Polycrystalline Germanium Thin Films"; pp. 326–31 in *Springer Proceedings in Physics*, Vol. 35. Edited by J. H. Werner, H. J. Moller, and H. P. Strunk. Springer-Verlag, Malente, Federal Republic of Germany, 1989.

[13] S. M. Sze, *Physics of Semiconductor Devices*. Wiley-Interscience, New York, 1969.

[14] C. H. Seager and T. G. Castner, "Zero Bias Resistance of Grain Boundaries in Neutron-Transmutation-Doped Polycrystalline Silicon," *J. Appl. Phys.*, **49** [7] 3879–89 (1978).

[15] G. E. Pike and C. H. Seager, "The dc Voltage Dependence of Semiconductor Grain-Boundary Resistance," *J. Appl. Phys.*, **50**, 3414 (1979).

[16] V. Srikant and D. R. Clarke; unpublished work.

[17] P. V. Evans and S. F. Nelson, "Determination of Grain Boundary Defect-State Densities from Transport Measurements," *J. Appl. Phys.*, **69** [6] 3605–11 (1991).

[18] W. Heywang, "Resistivity Anomaly in Doped Barium Titanate," *J. Am. Ceram. Soc.*, **47** [10] 484–90 (1964).

[19] G. H. Jonker, "Some Aspects of Semiconducting Barium Titanate, *Solid State Electron.*, **7**, 895–903 (1964). □